JOURNAL OF GUIDANCE, CONTROL, AND DYNAMICS
Vol. 15, No. 5, September-October 1992

Robust Flight Control Systems: A Parameter Space Design

Alberto Cavallo* and Giuseppe De Maria†
Università degli Studi di Napoli "Federico II," 80125 Naples, Italy
and
Leopoldo Verde‡
Centro Italiano Ricerche Aerospaziali, 81043 Capua, Italy

This paper deals with the longitudinal dynamics stabilization, around a trim condition, of an aircraft with unsatisfactory longitudinal stability characteristics. This problem is a single-input control problem because only elevator and canards deflections are used as control inputs, and they are simultaneously driven by the same control signal. To this aim, a new linear parameterization of all compensators stabilizing a given single-input plant is proposed, along with a design method based on a computationally tractable procedure for the robust stability analysis of polynomials with affinely dependent coefficient perturbations. Since scale factor sensor changes are perturbations entering affinely the characteristic polynomials coefficients of the closed-loop system, a controller will be synthesized in order to guarantee that the closed-loop poles lie in a specified domain of the complex plane prescribed by MIL specifications, and to achieve robustness against scale factor sensor failures. An application of the proposed procedure to the F4-E military aircraft is presented.

Nomenclature

a_n = normal acceleration, g
C_D = drag coefficient
C_L = lift coefficient
C_m = pitch moment coefficient
c = reference chord, m
g = acceleration of gravity, m/s^2
h = altitude, m
I_y = pitching moment of inertia, Kg m^2
m = mass of airplane, Kg
n_α = normal acceleration sensitivity with respect to angle of attack, g/rad
n_δ = normal acceleration sensitivity with respect to coupled elevator-canard deflection, g/rad
$\mathcal{P}^n$ = n-dimensional polynomial space
q = pitch rate, rad/s
$\bar{q}$ = dynamic pressure, N/m^2
$\boldsymbol{R}^n$ = n-dimensional Euclidean space
S = reference area, m^2
T = thrust, N
V = airspeed, m/s
$\|\boldsymbol{x}\|_\infty^w$ = weighted l_∞ norm of the vector $\boldsymbol{x}$, i.e., $\|\boldsymbol{x}\|_\infty^w = \max_i w_i|x_i|$, $w_i > 0$
α = angle of attack, rad
β = sideslip angle, rad
δ_c = canard deflection, rad
δ_{com} = input deflection command, rad
δ_e = elevator deflection, rad
ϑ = pitch attitude with respect to Earth, rad
ρ = air density, Kg/m^3
φ = roll attitude with respect to Earth, rad

Introduction

THE increased demand on aircraft performances asks for the use of more sophisticated control systems: e.g., aircraft with negative centering, trade reduced static stability for higher maneuvering capacities, and higher efficiency (reduction in fuel consumption). Because the aircraft is open-loop unstable, a stability augmentation system (SAS) is vital for its stabilization. Moreover, mere stability is not enough, and the added SAS must be designed to meet handling quality requirements.

By using linearized models of longitudinal- and lateral-directional closed-loop dynamics, with reference to a specified flight condition and to fixed values of aerodynamic, propulsive, inertial, structural, and controller parameters, the handling qualities are expressed in terms of desired pole location with an assigned tolerance in the complex plane (MIL-F-8785).

Since the values of these parameters are uncertain and the aircraft is highly vulnerable to incidents like failures of components (actuators, sensors, and flight computers), the SAS must be designed to achieve, for every flight condition within the flight envelope, robustness to off-nominal flight conditions and parameter uncertainties, and to provide fault tolerance against failures of components.

To meet these requirements for the closed-loop system, generally a hierarchical concept is used in the SAS design. The basic level consists of a controller (static or dynamic compensator) that, for a given flight condition, assigns closed-loop poles in specified regions of the complex plane according to handling quality specifications. The controller can be designed to meet robustness criteria with respect to off-nominal flight conditions, parameter uncertainties, and some kinds of sensor/actuator failures like changes in sensor scale factor and actuator gains. All of the more sophisticated tasks like failure detection and redundancy management, plant parameter identification, and controller scheduling are assigned to higher levels. For the active methods of fault tolerance one can refer to Refs. 1–4.

This paper deals with the longitudinal stability augmentation problem of an aircraft with inherent unsatisfactory longitudinal stability characteristics. As far as longitudinal dynamic stabilization around a trim condition is concerned, only elevator and canard deflections are used as control inputs (the engine thrust setting is supposed to be fixed). Moreover, since the elevator and canard deflections are simultaneously driven

Received April 23, 1991; revision received Nov. 11, 1991; accepted for publication Nov. 12, 1991.

*Ph.D. Student, Dipartimento di Informatica e Sistemistica, via Claudio 21.

†Associate Professor, Dipartimento di Informatica e Sistemistica, via Claudio 21.

‡Senior Researcher, Dipartimento di Meccanica del Volo e Controlli, via Maiorise.

by the same control signal, then the stabilization of the longitudinal dynamics is a single-input control problem.

To this aim, we propose a new parameterization of all compensators stabilizing a given single-input, multi-output plant, and a design method based on a computationally tractable robust stability test in plant parameter space with respect to assigned domain of the complex plane.[5,6]

A first characterization of all compensators stabilizing a given plant was introduced by Youla et al.[7] in 1976. Recently, in Ref. 8, the set of stabilizing compensators of assigned maximum order has been introduced for single-input, single-output plants. The design technique proposed in Ref. 8 allows the designer to assign closed-loop poles in specified domains of the complex plane and to meet other design specifications by using a specified number of degrees of freedom.

Moreover, in the very recent past, the automatic control literature has grown rich with new methodologies for the robust control system design both in the case of unstructured and structured plant parameter perturbations. For the former case, an exhaustive list of references can be found in Ref. 9. For the latter case, see Refs. 10 and 11. Recently, in Ref. 6, a new computationally tractable procedure for robust stability analysis of polynomials with linearly dependent coefficient perturbations has been proposed.

In this paper, we extend the result in Ref. 8 to single-input, multi-output plants, and by using the results in Refs. 5 and 6, we design a controller that assures handling quality specifications with assigned flight conditions inside the flight envelope; the resulting extra degress of freedom will be utilized in order to achieve robustness against scale factor sensor failures.

The paper is organized as follows. First, we introduce a new linear parameterization of all compensators stabilizing a given single-input plant. Second, we propose a design procedure in order to achieve robustness against multiplicative uncertainties. Finally, we present an application of the proposed technique to the longitudinal stabilization of the F4-E aircraft; the controller is designed in order to achieve robustness against scale factor sensor failures. Appendices A and B contain the proofs of the theorems enunciated in the first section.

All Stabilizing Compensators for Single-Input Plants

To introduce the control system design technique, some notations are necessary, and new results on all stabilizing compensators for single-input, multi-output systems are reported.

Consider the feedback system in Fig. 1 where $\boldsymbol{p}(s)$ and $\boldsymbol{c}(s)$ are given by

$$\boldsymbol{p}(s) = \frac{\boldsymbol{b}(s)}{a(s)}; \qquad \boldsymbol{b}(s) \in \mathcal{P}^r \tag{1}$$

$$\boldsymbol{c}(s) = \frac{\boldsymbol{x}^T(s)}{y(s)}; \qquad \boldsymbol{x}(s) \in \mathcal{P}^r \tag{2}$$

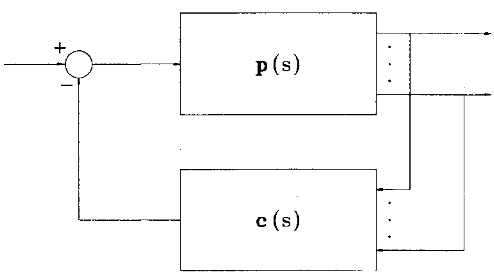

Fig. 1 Feedback system.

The transfer function of the feedback system in Fig. 1 is given by

$$\boldsymbol{W}(s) = \boldsymbol{p}(s)[1 + \boldsymbol{c}(s)\boldsymbol{p}(s)]^{-1}$$

$$= \frac{y(s)\boldsymbol{b}(s)}{y(s)a(s) + \boldsymbol{x}^T(s)\boldsymbol{b}(s)} = \frac{y(s)\boldsymbol{b}(s)}{d(s)} \tag{3}$$

In order to characterize the set of all stabilizing compensators, the general solution in terms of $y(s)$ and $\boldsymbol{x}(s)$ of the generalized diophantine equation

$$d(s) = y(s)a(s) + \boldsymbol{x}^T(s)\boldsymbol{b}(s) \tag{4}$$

must be provided. To do this, we introduce some preliminary notations.

The polynomials $a(s)$ and $y(s)$ can be expressed as

$$a(s) := a_1 + a_2 s + \cdots + a_{n+1}s^n = \boldsymbol{v}_n^T(s)\boldsymbol{a} \tag{5}$$

$$y(s) := y_1 + y_2 s + \cdots y_{\nu+1}s^\nu = \boldsymbol{v}_\nu^T(s)\boldsymbol{y} \tag{6}$$

where

$$\boldsymbol{v}_m^T(s) := (1 \; s \cdots s^m) \tag{7}$$

where $\boldsymbol{a}$ and $\boldsymbol{y}$ are the coefficient vectors of $a(s)$ and $y(s)$, respectively.

Now the product $a(s)y(s)$ can be expressed as follows:

$$a(s)y(s) = \boldsymbol{v}_{n+\nu}^T(s)\boldsymbol{S}_{\nu+1}(\boldsymbol{a})\boldsymbol{y} \tag{8}$$

where $\boldsymbol{S}_{\nu+1}(\boldsymbol{a})$ is the $(n + \nu + 1) \times (\nu + 1)$ Toeplitz matrix with first column $(\boldsymbol{a}^T, \boldsymbol{0}_\nu^T)^T$, i.e.,

$$\boldsymbol{S}_{\nu+1}(a) = \begin{bmatrix} a_1 & 0 & \cdots & 0 \\ \vdots & a_1 & \cdots & \vdots \\ a_{n+1} & \vdots & \ddots & \vdots \\ 0 & a_{n+1} & \ddots & a_1 \\ \vdots & 0 & \ddots & \vdots \\ 0 & 0 & & a_{n+1} \end{bmatrix} \tag{9}$$

Similarly, the polynomial vectors $\boldsymbol{b}(s)$ and $\boldsymbol{x}(s)$ can be expressed as

$$\boldsymbol{b}^T(s) = [b_1(s) \cdots b_r(s)]$$

$$= \boldsymbol{b}_1^T + \boldsymbol{b}_2^T s + \cdots + \boldsymbol{b}_{n+1}^T s^n = \boldsymbol{v}_n^T(s)\begin{pmatrix} \boldsymbol{b}_1^T \\ \vdots \\ \boldsymbol{b}_{n+1}^T \end{pmatrix} \tag{10}$$

$$\boldsymbol{x}(s) = [x_1(s) \cdots x_r(s)]^T$$

$$= \boldsymbol{x}_1 + \boldsymbol{x}_2 s + \cdots + \boldsymbol{x}_{\nu+1}s^\nu \tag{11}$$

where the meaning of the r-dimensional vectors $\boldsymbol{b}_i$, $i = 1, \ldots, n + 1$, and $\boldsymbol{x}_j$, $j = 1, \ldots, \nu + 1$ is obvious.

Now the product $\boldsymbol{b}^T(s)\boldsymbol{x}(s)$ can be written as follows:

$$\boldsymbol{b}^T(s)\boldsymbol{x}(s) = \boldsymbol{v}_{n+\nu}^T(s)\boldsymbol{S}_{\nu+1}(\boldsymbol{B})\boldsymbol{x} \tag{12}$$

where

$$\boldsymbol{B} = \begin{pmatrix} \boldsymbol{b}_1^T \\ \vdots \\ \boldsymbol{b}_{n+1}^T \end{pmatrix}, \qquad \boldsymbol{x} = \begin{pmatrix} \boldsymbol{x}_1 \\ \vdots \\ \boldsymbol{x}_{\nu+1} \end{pmatrix} \tag{13}$$

and $S_{\nu+1}(B)$ is the $(n + \nu + 1) \times (\nu + 1)r$ generalized Toeplitz matrix whose first r columns are $(B^T\ 0^T_{\nu\times r})^T$, i.e.,

$$S_{\nu+1}(B) = \begin{pmatrix} B & \begin{matrix} 0_r^T \\ B \\ \end{matrix} & \cdots & 0_{\nu\times r} \\ & & \cdots & \\ 0_{\nu\times r} & 0_{(\nu-1)\times r} & \cdots & B \end{pmatrix} \tag{14}$$

By using these notations, we can write the generalized diophantine equation (4) in the following alternative form:

$$[S_{\nu+1}(a)\ S_{\nu+1}(B)]\begin{pmatrix} y \\ x \end{pmatrix} = S\begin{pmatrix} y \\ x \end{pmatrix} = d \tag{15}$$

Now we formulate the following new theorem, whose proof is given in Appendix A.

Theorem 1. If $a_{n+1} \neq 0$, $a(s)$ and $b(s)$ are coprime, and $\nu \geq \nu_0 - 1$, where ν_0 is the observability index of a state realization of $b(s)/a(s)$, then

$$\text{rank}\ S = n + \nu + 1 \tag{16}$$

□

Theorem 1 allows us to solve the generalized diophantine equation (4) in terms of the compensator $c_\nu(s)$ of assigned order ν. Let $\mathcal{D}$ denote a set, not necessarily connected, in the complex plane. Then the set $\mathcal{C}$ of all stabilizing compensators $c_\nu(s)$ of order $\nu \geq \nu_0 - 1$, which ensures that the poles of the feedback system lie in the specified region $\mathcal{D}$, is given by

$$\mathcal{C} = \left\{ \frac{v_\nu^T(s)(B_1 d + B_2 z)}{v_\nu^T(s)(A_1 d + A_2 z)},\ d \in R_D^{n+\nu+1},\ z \in R^{(\nu+1)r-n} \right\} \tag{17}$$

Where $R_D^{n+\nu+1}$ denotes the set of vectors $d \in R^{n+\nu+1}$ such that the zeros of the associated polynomial $d(s)$ are in the region $\mathcal{D}$, and $z \in R^{(\nu+1)r-n}$ is the vector of completely free parameters.

The matrices A_1, B_1, A_2, B_2 are easily computed as follows. Denote with J the set of indexes of the first $n + \nu + 1$ linearly independent columns of the matrix S, and with T the following matrix:

$$T = \text{col}\{e_j\}, \qquad j \in J \tag{18}$$

where e_j is the $(\nu + 1)(r + 1)$ vector with 1 in jth position and 0 elsewhere, and col$\{e_j\}$ denotes the matrix whose columns are the vectors e_j, $j \in J$. Moreover, denote with $\bar{T}$ the matrix

$$\bar{T} = \text{col}\{e_k\}, \quad k \in \{1, \ldots, (\nu + 1)(r + 1)\} - J \tag{19}$$

Then by virtue of Theorem 1, the matrices A_1, B_1, A_2, B_2 are given by

$$\begin{pmatrix} A_1 \\ B_1 \end{pmatrix} = T(ST)^{-1} \tag{20}$$

$$\begin{pmatrix} A_2 \\ B_2 \end{pmatrix} = -T(ST)^{-1}S\bar{T} + \bar{T} \tag{21}$$

The steps leading to Eqs. (20) and (21) are detailed in Appendix B.

Robustness Against Plant Parameter Perturbations

The objective of this section is to design a compensator such that the closed-loop poles remain in a specified set $\mathcal{D}$ in the complex plane when the parameters vary in some set.

Consider an uncertain plant, i.e., $a(s)$ and $b(s)$ depend on some parameters k, and assume that the coefficients of $a(s)$ and $b(s)$ depend affinely on k.

With reference to Fig. 1, the closed-loop characteristic polynomial can be written as

$$d_\nu(s, z, k) = a(s, k)y(s, z) + x^T(s, z)b(s, k) \tag{22}$$

where

$$c_\nu(s, z) = \frac{x^T(s, z)}{y(s, z)} \in \mathcal{C} \tag{23}$$

has been designed to assure a prescribed closed-loop pole location when the parameters assume their nominal values.

Denote with $\mathcal{K}$ the parameter space, with $\bar{k}$ the vector of nominal parameters, and with $\mathcal{K}_D$ the $\mathcal{D}$-stability region in the $\mathcal{K}$ space with a given compensator $c_\nu(s, z)$,

$$\mathcal{K}_D = \{k \mid d(z, k) \in R_D^{n+\nu+1}\} \tag{24}$$

A neighborhood $\mathcal{H}(\bar{k}, \rho)$ of $\bar{k}$ can be defined by

$$\mathcal{H}(\bar{k}, \rho) = \{k \mid \|k - \bar{k}\|_\infty^w < \rho\} \tag{25}$$

Now the goal of this section can be stated as follows: select a compensator in the set $\mathcal{C}$ that allows us to enlarge the neighborhood $\mathcal{H}(\bar{k}, \rho)$ to the maximum extent with the constraint that the poles of the closed-loop system belong to $\mathcal{D}$ for any $k \in \mathcal{H}(\bar{k}, \rho)$.

This can be accomplished by solving the following problems.

Problem A:

$$\bar{\rho}(z, \bar{k}) = \sup \rho$$
$$\text{subject to} \begin{cases} \|k - \bar{k}\|_\infty^w < \rho \\ d(z, k) \in R_D^{n+\nu+1} \end{cases} \tag{26}$$

Problem B:

$$\rho_\nu^0(\bar{k}) = \max_z \bar{\rho}(z, \bar{k})$$

The crucial point in solving problem A is to test condition (26), whereas the solution of problem B depends on the choice of the weighting vector w. Note that an optimum vector w cannot be selected a priori, but some attempts are necessary to choose the best w that allows us to enlarge the neighborhood $\mathcal{H}(\bar{k}, \rho)$ to the maximum extent. As the closed-loop characteristic polynomial coefficients depend affinely on k, the image in the coefficient space of the neighborhood (25) is a polytope with m vertices at the most, where m is the number of vertices of the neighborhood (25). By denoting with

$$d_i(z) = d(z, k_i), \qquad i = 1, \ldots, m \tag{27}$$

the vertices of such a polytope, where k_i is the ith vertex of the hyper-rectangle $\|k - \bar{k}\|_\infty^w < \rho$, condition (26) can be rewritten as

$$\sum_{i=1}^{m} \lambda_i d_i(z) \in R_D^{n+\nu+1}, \qquad \lambda_i \geq 0, \qquad \sum_{i=1}^{m} \lambda_i = 1 \tag{28}$$

Note that the number of vertices of the polytope in the coefficient space is generally less than m, but to simplify computations, we may assume the vectors $d_i(z)$ to be the image of the vertices k_i.

This condition can be tested by using an efficient stability test proposed in Ref. 6, which is based on the following Theorem.

Theorem 2. Let a family of polynomials $d(s, z)$ be the convex combination of m assigned monic polynomials $d_i(s, z)$, $i = 1$,

$\ldots, m$. Consider a region $\mathcal{D}$, not necessarily connected, in the complex plane, denote with $\partial\mathcal{D}$ the boundary of $\mathcal{D}$, and suppose that at least one polynomial of the family is $\mathcal{D}$ stable. Then all of the roots of the family $d(s, z)$ are inside $\mathcal{D}$ if and only if the following conditions hold

$$\text{a)}\quad d_i(\hat{s}, z) \neq 0, \qquad \forall \hat{s} \in \partial\mathcal{D} \tag{29}$$

$$\text{b)}\quad \sup_{\hat{s} \in \partial\mathcal{D}} |\phi_\theta(d_i(\hat{s},z)) - \phi_\theta(d_j(\hat{s},z))| < \pi$$

$$\theta = \arg(d_1(\hat{s}, z)), \quad \forall i, \ j = 2, \ldots, m, \quad i > j \tag{30}$$

where $\phi_\theta(\chi)$, $\theta \in [-\pi, \pi)$, denotes the main argument of $\chi e^{-j\theta}$. □

The proof of Theorem 2 can be found in Ref. 6.

Since the nominal closed-loop polynomial belongs to the $\mathcal{D}$-stability region, then the test Eqs. (29) and (30) and an univariate minimization algorithm, such as bisection or golden section search, can be easily used to solve problem A.

As concerns problem B, note that, since nothing is known about the convexity of the function $\bar{\rho}_\nu(z, \bar{k})$, there is no guarantee that a global maximum will be found. A common procedure in such cases is to choose several initial guesses, attempt to find local optimum, and to then select the best workable answer.

The solution of problem B gives a vector $\bar{z}$ and a compensator $c_\nu(s, \bar{z})$, which allows the closed-loop system to tolerate the largest parameter variation according to the selected norm and region $\mathcal{D}$.

By using this procedure, it is possible to give an estimate of the real $\mathcal{D}$-stability region in the $\mathcal{K}$ plane. To this end, denote by $\mathcal{H}^0(\bar{k})$ the largest neighborhood of $\bar{k}$:

$$\mathcal{H}^0(\bar{k}, \rho) = \{k \mid \|k - \bar{k}\|_\infty^w < \rho_\nu^0(\bar{k})\} \tag{31}$$

It is easy to show that by varying $\bar{k}$ it is possible to build a sequence of sets that converges to $\mathcal{K}_D$; each set is made by unions of neighborhoods $\mathcal{H}^0(k^*)$:

$$\mathcal{K}_D(n) = \bigcup_{k^* \in \mathcal{K}_D(n-1)} \mathcal{H}^0(k^*),$$

$$n \in N, \quad \mathcal{K}_D(1) = \mathcal{H}^0(\bar{k}) \tag{32}$$

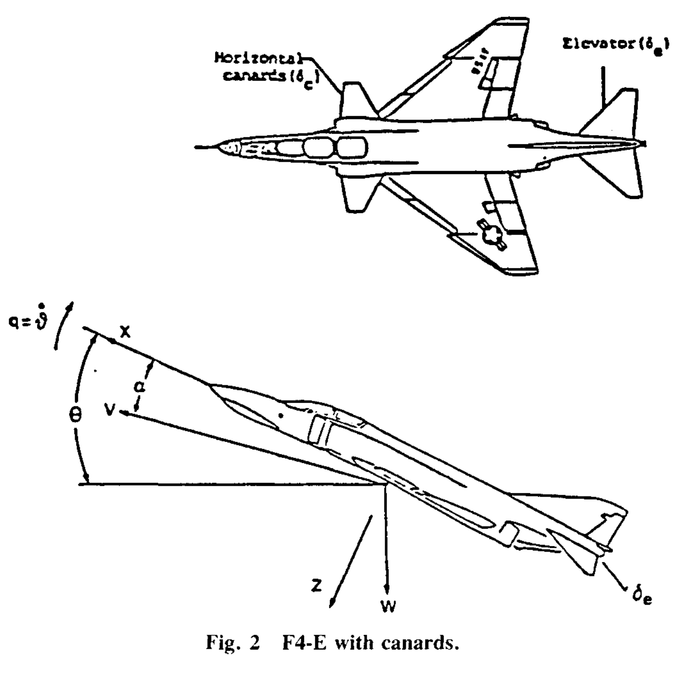

Fig. 2 F4-E with canards.

then

$$\lim_n \mathcal{K}_D(n) = \mathcal{K}_D \tag{33}$$

Obviously, from a practical point of view, it is impossible to obtain the exact region via Eq. (33), but generally a good estimate of $\mathcal{K}_D$ suffices. Moreover when $\lim k = 2$ the neighborhood (25) is a rectangle and the solution can be easily represented pictorially. In the next section, we will show how, by a suitable selection of the point k^*, it is possible to achieve an adequate estimate of $\mathcal{K}_D$ with few rectangles.

As concerns the compensator order, it is possible to show that, by increasing ν, a larger, or at least not smaller, $\mathcal{D}$-stability region $\mathcal{K}_D$ can be obtained. In fact, since the proposed parametrization is complete, it is always possible to obtain any compensator of order ν by pole-zero cancellation on a compensator of order $\nu + 1$. Hence, with a compensator of order $\nu + 1$, by solving problem B, we at least obtain $\rho_{\nu+1}^0(\bar{k}) = \rho_\nu^0(\bar{k})$.

Keeping this in mind, we can start the random-search procedure to solve problem B for a ν-order compensator from a vector $\bar{\bar{z}}$ such that

$$c_\nu(s, \bar{\bar{z}}) = c_{\nu-1}(s, \bar{z}) \tag{34}$$

By considering that $\bar{T}^T \bar{T} = I$ and $\bar{T}^T T = 0$, it is easy to show that the vector $\bar{\bar{z}}$ is given by

$$\bar{\bar{z}} = \bar{T}^T \begin{pmatrix} 0_{\nu+1,2} \\ \hline \bar{S}(\beta^{(\nu-1)}) \end{pmatrix} \begin{pmatrix} \gamma \\ 1 \end{pmatrix} \tag{35}$$

where $-\gamma$ is the farther pole of the closed-loop system, i.e., $d_\nu(s, \bar{k}) = d_{\nu-1}(s, \bar{k})(s + \gamma)$, $x^{(\nu-1)}$ is the vector of the $(\nu - 1)$-order compensator numerator coefficients, and $\bar{S}(x^{(\nu-1)})$ is the $r(\nu + 1) \times 2$ matrix

$$\bar{S}(x^{(\nu-1)}) = \begin{bmatrix} x_{11} & 0 \\ x_{12} & 0 \\ \vdots & \vdots \\ x_{1r} & 0 \\ x_{21} & x_{11} \\ x_{22} & x_{12} \\ \vdots & \vdots \\ x_{2r} & x_{1r} \\ \vdots & \vdots \\ 0 & x_{\nu 1} \\ 0 & x_{\nu 2} \\ \vdots & \vdots \\ 0 & x_{\nu 2} \end{bmatrix} \tag{36}$$

In the following section, this procedure will be used to determine the sensor redundancy degree to achieve fault tolerance.

Case Study

Model

We refer to the F4-E aircraft as in the work of Ackermann.[12,13] The F4-E is a military aircraft that is destabilized by horizontal canards (Fig. 2). The aircraft is unstable in subsonic flight and unsufficiently damped in supersonic flight, then adequate handling qualities must be provided by the control system.

In the following, we briefly outline the decoupled longitudinal equations of the motion of an aircraft. Most aircraft dynamics texts (e.g., Refs. 14 and 15), give more detailed versions of the derivation of these equations.

In the polar coordinate velocity form, the nonlinear equations of the longitudinal motion of the rigid aircraft, symmetrical with respect to X-Z plane (Fig. 2) and flying at small sideslip and roll angles, can be written as follows

$$\dot{\alpha} = -\frac{\overline{q}S}{mV}C_L + q + \frac{g}{V}\cos(\vartheta - \alpha) - \frac{T\sin\alpha}{mV} \tag{37}$$

$$\dot{V} = -\frac{\overline{q}S}{m}C_D + g\sin(\alpha - \vartheta) + \frac{T}{m}\cos\alpha \tag{38}$$

$$\dot{q}I_y = \overline{q}ScC_m \tag{39}$$

$$\dot{\vartheta} = q \tag{40}$$

where $\overline{q} = \rho V^2/2$ is the dynamic pressure, and the air density ρ can be expressed as $\rho = \rho(h)$.

Assuming that the normal acceleration a_n and pitch rate q are available measurements by using one accelerometer and one gyro, respectively, the output equations can be written as

$$\begin{pmatrix} a_n \\ q \end{pmatrix} = \begin{bmatrix} \overline{q}S(C_L\cos\alpha + C_D\sin\alpha)/mg - \cos\vartheta \\ q \end{bmatrix} \tag{41}$$

As far as longitudinal dynamics control devices are concerned, it is supposed that, in each flight condition within the airplane flight envelope, only elevator and canard deflections are used to control the longitudinal dynamics around the steady condition. This means that in the meantime the engine thrust setting is supposed to be fixed.

Moreover, the elevator and canard are not used independently in stationary flight, i.e., the commanded deflections are coupled: $\delta_c = K_c\delta_e$ (Fig. 3), where the factor K_c is chosen for each flight condition in order to achieve minimum drag combination of canard and elevator deflections. Thus, the longitudinal dynamics stabilization is a single-input problem.

In Fig. 3, the open-loop system, including a first-order low-pass actuator dynamics with time constant τ, is represented.

For each trim flight condition within the flight envelope of the airplane, the model obtained by linearizing the nonlinear equations (37–41), for small perturbations about trim condition, including actuator dynamics and elevator-canard deflections coupling, can be written as

$$\frac{\mathrm{d}}{\mathrm{d}t}\begin{pmatrix} \alpha \\ q \\ V \\ \vartheta \\ \delta_e \end{pmatrix} = \begin{pmatrix} Z_\alpha & 1 & Z_V & -\sin(\vartheta - \alpha)g/V & Z_\delta \\ M_\alpha & M_q & M_V & 0 & M_\delta \\ X_\alpha & 0 & X_V & -g\cos(\vartheta - \alpha) & X_\delta \\ 0 & 1 & 0 & 0 & 0 \\ 0 & 0 & 0 & 0 & -1/\tau \end{pmatrix}\begin{pmatrix} \alpha \\ q \\ V \\ \vartheta \\ \delta_e \end{pmatrix} + \begin{pmatrix} 0 \\ 0 \\ 0 \\ 0 \\ 1/\tau \end{pmatrix}\delta_{\mathrm{com}} \tag{42}$$

$$\begin{pmatrix} a_n \\ q \end{pmatrix} = \begin{pmatrix} n_\alpha & 0 & 0 & \sin\vartheta & n_\delta \\ 0 & 1 & 0 & 0 & 0 \end{pmatrix}\begin{pmatrix} \alpha \\ q \\ V \\ \vartheta \\ \delta_e \end{pmatrix} \tag{43}$$

where $M_{(\cdot)}$, $X_{(\cdot)}$, $Z_{(\cdot)}$ are the longitudinal dimensional stability and control derivatives, and M_δ, X_δ, Z_δ are the sum of the corresponding derivative with respect to δ_e and K_c times the corresponding derivative with respect to δ_c.

Stability Augmentation System Design

Generally, high-performance requirements in terms of better efficiency (reduction in fuel consumption) and maneuverability impose intrinsic instability on the aircraft. Then, an

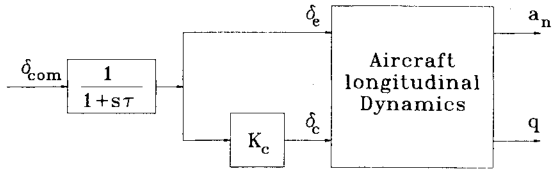

Fig. 3 Open-loop system.

Table 1 Limits for ζ and ω_n

Short period		Phugoid
ζ_{sp}	ω_{nsp}	ζ_p
0.35–1.3	3.5–12.6	≥0.04

SAS is required for its stabilization. Moreover, airworthiness rules [MIL-F-8785 (ASG), 1969] require that the aircraft is safely controllable by the pilot without any exceptional piloting skill. These requirements deal with the dynamic aircraft behavior and are referred to in literature as handling qualities.

With reference to the assigned flight condition, the handling qualities are expressed in terms of admissible ranges of variation for damping coefficients ($\zeta_{\min}$, $\zeta_{\max}$) and natural frequencies ($\omega_{\min}$, $\omega_{\max}$) of the rigid-body modes associated with the linearized model (42) and (43) (short period and phugoid modes). Then the SAS design problem can be formulated as follows. Design a control system that has the following properties:

1) It assures that the closed-loop poles lie in the prescribed region of the complex plane; for instance, for category A flight phase, with steady-state normal acceleration sensitivity with respect to angle of attack n_α = 50 g/rad, corresponding to the flight condition h = 5000 ft, Mach = 0.85 for the F4-E military aircraft, the limits imposed by MIL specs are reported in Table 1.

2) It provides some kind of fault tolerance against incidents like sensor failures.

3) It improves robustness with respect to off-nominal flight conditions and plant uncertainty parameters.

Suppose that the linearized model of longitudinal dynamics for an assigned flight condition is available. Then in order to meet requirements 1 and 2, a compensator of suitable order ν can be designed by means of Eq. (17) so that all of the closed-loop poles lie in the region $\mathcal{D}$ of the complex plane prescribed by the MIL specs ($\mathcal{D}$ stability), and there are a suitable number of degrees of freedom in order to ensure robustness against sensor scale factor changes. Indeed, the procedure illustrated earlier can be applied to achieve robustness against all perturbations entering affinely the coefficients of the closed-loop characteristic polynomial. As concerns requirement 3, off-nominal flight conditions and uncertainities on stability derivatives are perturbations entering nonlinearly, then a different design method must be adopted. A first approximate design procedure can be found in Refs. 16 and 17.

Robustness Against Scale Factor Sensor Failures

Now we refer to the sensor scale factor failure problem, which can be viewed as a robust stability problem of a linear dynamical system with structured linear perturbations.

According to previous terminology, $\bar{\boldsymbol{k}}$ denotes the vector of nominal sensor gains, $\bar{\boldsymbol{k}} = (K_{a_n}, K_q)^T$. Then Eq. (22) becomes

$$d_\nu(s, z, \boldsymbol{k}) = a(s)y(s, z) + \boldsymbol{x}^T(s, z)\,\mathrm{diag}\{K_{a_n}, K_q\}\boldsymbol{b}(s) \tag{44}$$

Now, a failure of the accelerometer or of the gyro is equivalent to a reduction of the respective gain, K_{a_n} or K_q, from the nominal values to zero.

We say that $c_\nu(s, z)$ achieves robustness against a failure of the accelerometer (gyro) if the projection of $\bar{k}$ on the axis $K_{a_n} = 0$ ($K_q = 0$) is contained in $\mathcal{H}_D$, where $\mathcal{D}$ is selected according to MIL specs (Fig. 4).

Analogously, we say that $c_\nu(s, z)$ has a $100/n\%$ gain reduction margin in K_{a_n} (K_q) if the projection of $\bar{k}$ on the line $K_{a_n} = \bar{K}_{a_n}/n$ ($K_q = \bar{K}_q/n$) is contained in $\mathcal{H}_D$.

Note that robustness against scale factor sensor changes can be achieved by a compensator with $100/n\%$ gain reduction margin by using an n-redundant sensor system (the parallel of n sensors each with nominal gain equals to the full nominal gain divided by n).

To compare the results obtained with the proposed procedure with that in Refs. 12 and 13, the same simplified third-order model, including the short-period longitudinal mode and actuator dynamics in sensor coordinates is considered.

Indeed, it can be shown[18] that the forward velocity V has only a negligible influence on the short-period mode of the aircraft. Furthermore, the relation between pitch angle and pitch rate is purely a kinematical one. Therefore, we can simplify the state vector Eqs. (42) and (43) describing only the short-period mode of the aircraft dynamics

$$\frac{\mathrm{d}}{\mathrm{d}t}\begin{pmatrix}\alpha\\ q\\ \delta_e\end{pmatrix} = \begin{pmatrix}Z_\alpha & 1 & Z_\delta\\ M_\alpha & M_q & M_\delta\\ 0 & 0 & -1/\tau\end{pmatrix}\begin{pmatrix}\alpha\\ q\\ \delta_e\end{pmatrix} + \begin{pmatrix}0\\ 0\\ 1/\tau\end{pmatrix}\delta_{\mathrm{com}} \tag{45}$$

$$\begin{pmatrix}a_n\\ q\end{pmatrix} = \begin{pmatrix}n_\alpha & 0 & n_\delta\\ 0 & 1 & 0\end{pmatrix}\begin{pmatrix}\alpha\\ q\\ \delta_e\end{pmatrix} \tag{46}$$

Based on the output equation (46), a linear transformation on the state equation (45) leads the following state equation in sensor coordinates.

$$\frac{\mathrm{d}}{\mathrm{d}t}\begin{pmatrix}a_n\\ q\\ \delta_e\end{pmatrix} = \begin{pmatrix}Z_\alpha & n_\alpha & -n_\delta Z_\alpha + n_\alpha Z_\delta - n_\delta/\tau\\ M_\alpha/n_\alpha & M_q & -n_\delta M_\alpha/n_\alpha + M_\delta\\ 0 & 0 & -1/\tau\end{pmatrix}\begin{pmatrix}a_n\\ q\\ \delta_e\end{pmatrix} + \begin{pmatrix}n_\delta/\tau\\ 0\\ 1/\tau\end{pmatrix}\delta_{\mathrm{com}} \tag{47}$$

With reference to the subsonic cruise flight condition (Mach = 0.85, h = 5000 ft), the aerodynamic data are listed in Table 2.

The MIL specs for the short period mode in the specified flight condition are

$$3.50 \le \omega_{n_{\mathrm{sp}}} \le 12.6, \qquad 0.35 \le \zeta_{\mathrm{sp}} \le 1.3 \tag{48}$$

The poles added by the actuator and the compensator must belong to a region characterized by

$$12.6 < \omega_n \le 70, \qquad \zeta \ge 0.35 \tag{49}$$

the upper ω_n constraint is chosen in order to maintain a bandwidth limitation below the first structural mode frequency.

Table 2 Aerodynamic data for the F4-E[a]

Z_α	−1.702 (1/s)
M_α	11.163 (1/s²)
M_q	−1.418 (1/s)
Z_δ	0.481 (1/s)
M_δ	−36.269 (1/s²)
n_α	50.72 (g/rad)
n_δ	−19.433 (g/rad)
K_c	−0.7
τ	1/14 (s)

[a]Mach = 0.85; altitude = 5000 ft.

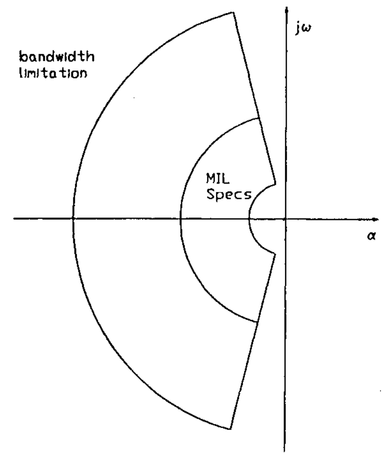

Fig. 4 $\mathcal{D}$-stability region in the complex plane.

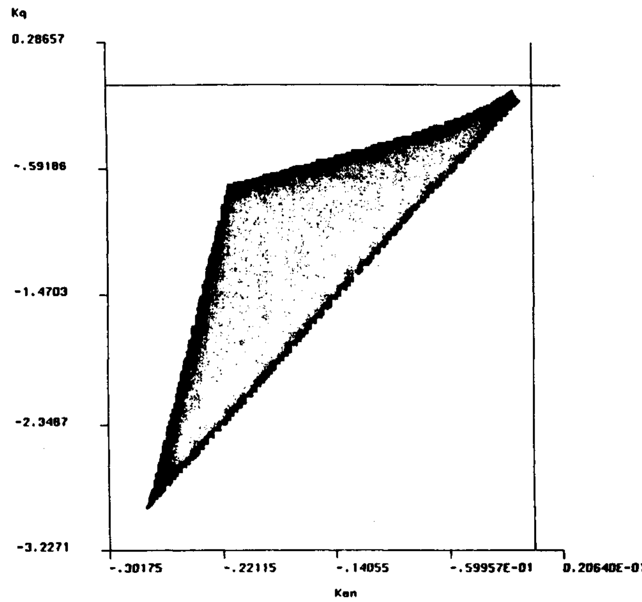

Fig. 5 $\mathcal{D}$-stability region in sensor gain plane, $\nu = 0$.

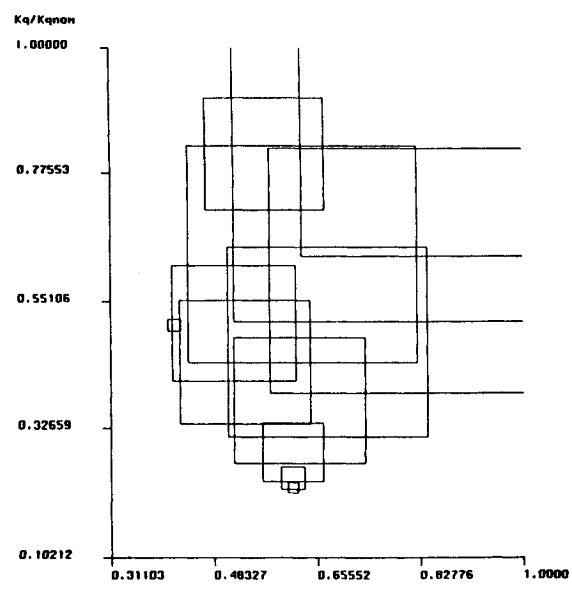

Fig. 6 $\mathcal{D}$-stability region in sensor gain plane, $\nu = 1$.

Figure 4 shows the region $\mathcal{D}$ in the complex plane corresponding to these requirements.

In Fig. 5, the stability region in the sensor gain space, in the case $\nu = 0$ (static compensator), is reported. The picture

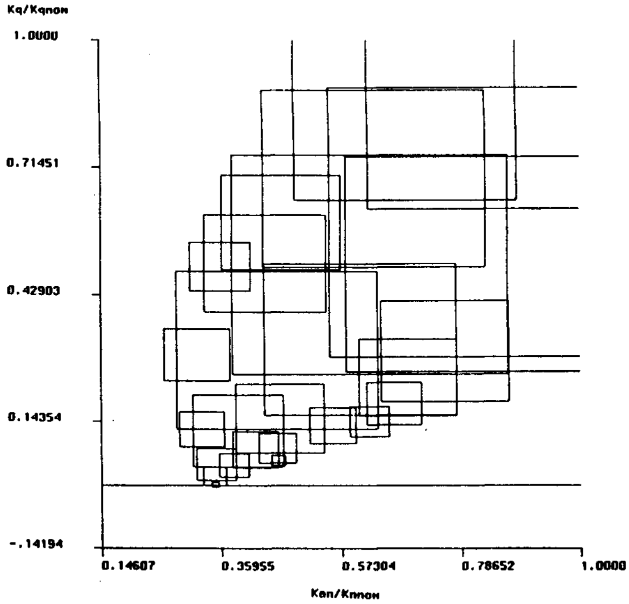

Fig. 7 $\mathcal{D}$-stability region in sensor gain plane, $\nu = 2$.

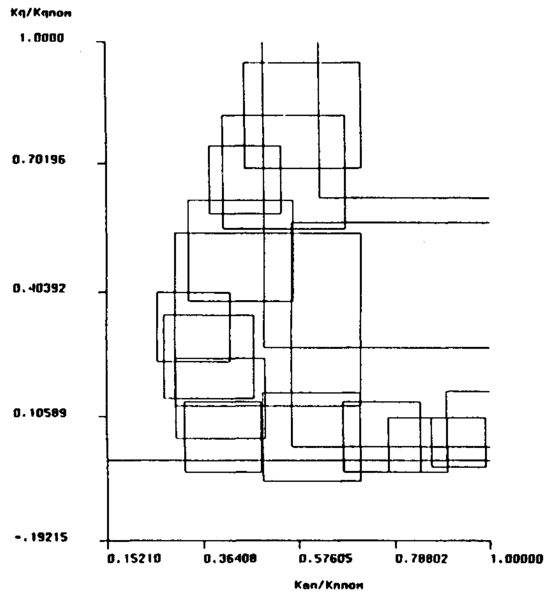

Fig. 8 $\mathcal{D}$-stability region in sensor gain plane, $\nu = 2$ (relaxed specs).

has been obtained by drawing about 300 rectangles and then painting the interior of the region to easily visualize its boundary. The stability region coincides with that in Ref. 12.

In Fig. 6, the case $\nu = 1$ is illustrated. In this case, one degree of freedom is available in order to solve optimization problem B. The value $\bar{z} = -1.2$ has been selected. The axes have been normalized. As one can see, the system is tolerant to an independent reduction of 50% in sensor gains. Then a two-redundant sensor system is sufficient to achieve fault tolerance. The picture has been done with a small number of rectangles, as we are not interested in the exact region, but an estimate suffices. The most interesting points are those close to the axes, and so the strategy adopted has been to move the center $\boldsymbol{k}^*$ of the neighborhoods toward the axes.

In Fig. 7, the case $\nu = 2$ is illustrated. In this case, three degrees of freedom are available. The vector z, which assures the best local maximum in problem B, is

$$z = (-69.41 \quad -0.1173 \quad -2.4785)^T \tag{50}$$

This value has been obtained by starting the optimization procedure from the value $\bar{\bar{z}}$ such that $c_1(s, \bar{z}) = c_2(s, \bar{\bar{z}})$, where $\bar{\bar{z}}$ is given by Eq. (35). Figure 7 shows that the second-order compensator, in addition to the fault tolerance properties of the first-order compensator, allows the sensor gain K_q to reduce to zero if K_{a_n} assumes the value 0.32.

If relaxed specs can be temporarily assumed ($0.14 \leq \zeta_{sp} \leq 1.3$), then the high-level control system can select the specified value of $K_{a_n} = 0.32$. This case is illustrated in Fig. 8.

Simulation results showing the transient behavior following a sudden scale factor change are reported in Figs. 9–11. We suppose that a disturbance gw acts on the normal acceleration and in the meantime a sudden reduction of the accelerometer and gyro scale factors happens at $t = 4$ s. In Fig. 9, the case $\nu = 2$ and a 50% reduction of both sensors is reported. In Figs. 10 and 11, the cases of 100% reduction in K_q, $\nu = 0$ and $\nu = 2$, respectively, are reported.

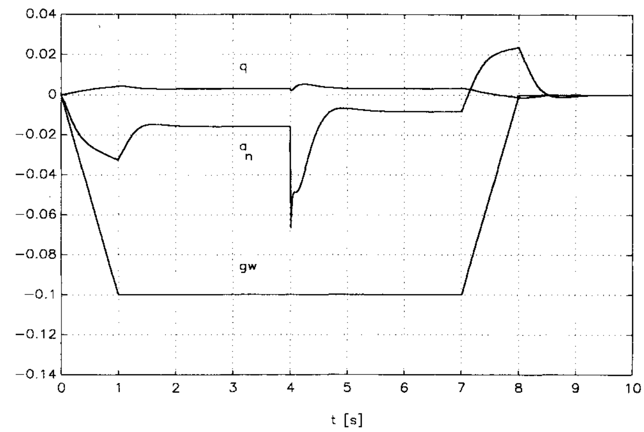

Fig. 9 Transient response with 50% of sensor gains, $\nu = 2$.

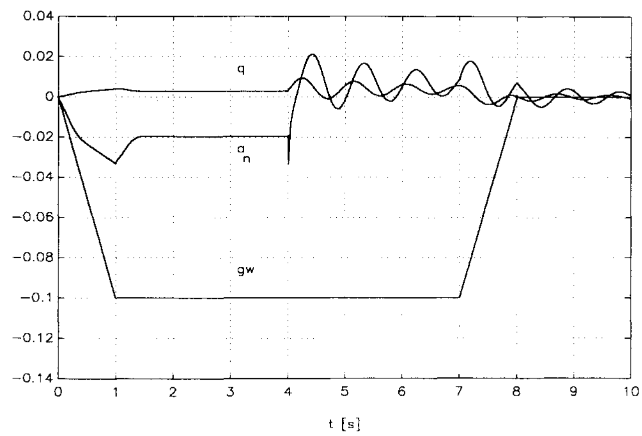

Fig. 10 Transient response, $K_q = 0$, $\nu = 0$.

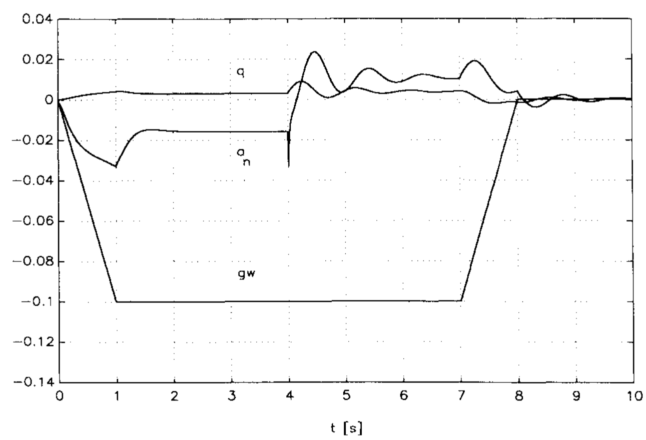

Fig. 11 Transient response, $K_q = 0$, $\nu = 2$.

Remark. The result obtained in this application is due to the fact that the plant has no zeros in the right half-plane, as can be easily verified. The procedure presented here does not show anything about the maximum improvement in robustness achievable, it just tries to enlarge the region in the parameter space at each step. It is well known that if a plant has right half-plane zeros it is intrinsically restricted in achievable robustness. Then, in this case, by increasing the compensator order, no further improvement will be obtained.

Conclusions

In this paper, a new linear parameterization of all stabilizing compensators for single-input, multi-output systems has been proposed. Such a parametrization allows the designer to assign closed-loop poles in specific domains of the complex plane and to meet other design specifications by using a specified number of degrees of freedom. By using a computationally tractable procedure for the robust stability analysis of polynomial with linearly dependent coefficient perturbations, a design method has been proposed that allows the closed-loop system to achieve robustness against scale factor sensor failures. A case study has been carried out with reference to the F4-E military aircraft, and simulation results showing the transient behavior following a sudden scale factor change have also been reported.

Appendix A

The proof of Theorem 1 uses the following results.

Lemma 1. If

$$a(s) = \boldsymbol{v}_n^T(s)\boldsymbol{a} = \boldsymbol{v}_{n-1}^T(s)\hat{\boldsymbol{a}} + a_{n+1}s^n \tag{A1}$$

$$\boldsymbol{b}^T(s) = \boldsymbol{v}_n^T(s)\boldsymbol{B} = \boldsymbol{v}_{n-1}^T(s)\hat{\boldsymbol{B}} + \boldsymbol{b}_{n+1}^T s^n \tag{A2}$$

are coprime polynomials, then

$$a'(s) = \boldsymbol{v}_n^T(s)\boldsymbol{a}' = \boldsymbol{v}_{n-1}^T(s)\hat{\boldsymbol{a}}' + s^n \tag{A3}$$

$$\boldsymbol{b}'^T(s) = \boldsymbol{v}_n^T(s)\boldsymbol{B}' = \boldsymbol{v}_{n-1}^T(s)\hat{\boldsymbol{B}}' \tag{A4}$$

where

$$\boldsymbol{a}' = \boldsymbol{a}/a_{n+1}, \qquad \boldsymbol{B}' = \boldsymbol{B} - \boldsymbol{a}'\boldsymbol{b}_{n+1}^T \tag{A5}$$

are coprime polynomials.

Proof. If $\hat{s}$ is such that $a(\hat{s}) = 0$, by hypothesis $\boldsymbol{b}(\hat{s}) \neq 0$, then it follows that

$$a'(\hat{s}) = 0, \qquad \boldsymbol{b}'(\hat{s}) = \boldsymbol{b}(\hat{s}) \neq 0 \tag{A6}$$

□

Lemma 2. If

$$a'(s) = \boldsymbol{v}_{n-1}^T(s)\hat{\boldsymbol{a}}' + s^n \tag{A7}$$

$$\boldsymbol{b}'^T(s) = \boldsymbol{v}_{n-1}^T(s)\hat{\boldsymbol{B}}' \tag{A8}$$

are coprime polynomials, then

$$\text{rank}\ (\hat{\boldsymbol{B}}'\ \hat{\boldsymbol{A}}'\hat{\boldsymbol{B}}' \cdots \hat{\boldsymbol{A}}'^{\nu}\hat{\boldsymbol{B}}') = n, \qquad \forall \nu \geq \nu_r - 1 \tag{A9}$$

Where ν_r is the reachability index of the pair $(\hat{\boldsymbol{A}}', \hat{\boldsymbol{B}}')$ and

$$\hat{\boldsymbol{A}}' = \left(\begin{array}{c|c} \boldsymbol{0}^T & \\ \hline \boldsymbol{I}_{n-1} & -\hat{\boldsymbol{a}}' \end{array}\right) \tag{A10}$$

denotes the right vertical companion matrix defined by the vector $\hat{\boldsymbol{a}}'$. □

Proof. It is well known that, if $a'(s)$ and $\boldsymbol{b}'(s)$ are coprime, then the pair $(\hat{\boldsymbol{A}}', \hat{\boldsymbol{B}}')$ is reachable. □

Remark (A1). Since the dynamical matrix and the output matrix for the observed variables of the state realization of $\boldsymbol{b}(s)/a(s)$ in controllability form are, as can be easily verified, $\hat{\boldsymbol{A}}'^T$ and $\hat{\boldsymbol{B}}'^T$, respectively, then, by duality, Eq. (A9) holds for each $\nu \geq \nu_0 - 1$, where ν_0 is the observability index of the state realization of $\boldsymbol{b}(s)/a(s)$. □

Proof of Theorem 1. By means of the elementary transformations (A5), we obtain the matrix

$$[\boldsymbol{S}_{\nu+1}(\boldsymbol{a}')\ \boldsymbol{S}_{\nu+1}(\boldsymbol{B}')]$$

$$= \begin{bmatrix} a_1' & 0 & \cdots & 0 & \hat{\boldsymbol{B}}' & \boldsymbol{0}^T & \cdots & \boldsymbol{0}^T \\ a_2' & a_1' & \cdots & 0 & \boldsymbol{0}^T & \hat{\boldsymbol{B}}' & \cdots & \vdots \\ \vdots & \vdots & \ddots & \vdots & \vdots & \vdots & \ddots & \vdots \\ a_n' & \vdots & \cdots & a_1' & \vdots & \vdots & \cdots & \vdots \\ 1 & a_n' & \cdots & \vdots & \vdots & \vdots & \cdots & \vdots \\ 0 & 1 & \cdots & \vdots & \vdots & \vdots & \cdots & \vdots \\ \vdots & \vdots & \ddots & \vdots & \vdots & \vdots & \cdots & \vdots \\ 0 & 0 & \cdots & 1 & \boldsymbol{0}^T & \boldsymbol{0}^T & \cdots & \hat{\boldsymbol{B}}' \end{bmatrix} \tag{A11}$$

Note that

$$(\hat{\boldsymbol{B}}'\ \hat{\boldsymbol{A}}'\hat{\boldsymbol{B}}' \cdots \hat{\boldsymbol{A}}'^{\nu}\hat{\boldsymbol{B}}') = (\hat{\boldsymbol{B}}^{(0)}\ \hat{\boldsymbol{B}}^{(1)} \cdots \hat{\boldsymbol{B}}^{(\nu)}) \tag{A12}$$

where

$$\hat{\boldsymbol{B}}^{(0)} = \hat{\boldsymbol{B}}'$$

$$\hat{\boldsymbol{B}}^{(i)} = \begin{pmatrix} \boldsymbol{b}_1^{T(i)} \\ \boldsymbol{b}_2^{T(i)} \\ \vdots \\ \boldsymbol{b}_n^{T(i)} \end{pmatrix} = \begin{pmatrix} \boldsymbol{0}^T \\ \boldsymbol{b}_1^{T(i-1)} \\ \vdots \\ \boldsymbol{b}_{n-1}^{T(i-1)} \end{pmatrix} - \boldsymbol{b}_n^{T(i-1)} \begin{pmatrix} a_1' \\ a_2' \\ \vdots \\ a_n' \end{pmatrix} \tag{A13}$$

By means of the elementary transformation (A13) on the columns of $\boldsymbol{S}_{\nu+1}(\hat{\boldsymbol{B}}')$, we obtain the matrix

$$\boldsymbol{S}' = \left[\begin{array}{cccc|c} a_1' & 0 & \cdots & 0 & \\ a_2' & a_1' & \cdots & \vdots & \hat{\boldsymbol{B}}'\ \hat{\boldsymbol{A}}'\hat{\boldsymbol{B}}' \cdots \hat{\boldsymbol{A}}'^{\nu}\hat{\boldsymbol{B}}' \\ \vdots & \vdots & \cdots & \vdots & \\ a_n' & a_{n-1}' & \cdots & a_1' & \\ \hline 1 & a_n' & \cdots & \vdots & \\ 0 & 1 & \cdots & \vdots & \boldsymbol{0} \\ \vdots & \vdots & \cdots & a_n' & \\ 0 & 0 & \cdots & 1 & \end{array}\right] \tag{A14}$$

It is easy to verify that

$$\text{rank}(\boldsymbol{S}) = \text{rank}(\boldsymbol{S}') = n + \nu + 1 \tag{A15}$$

then, taking into account Remark A1, the proof is complete. □

Appendix B

To obtain Eqs. (20) and (21), note that by definition $\boldsymbol{T}$ and $\bar{\boldsymbol{T}}$ satisfy the following identity

$$\boldsymbol{T}\boldsymbol{T}^T + \bar{\boldsymbol{T}}\bar{\boldsymbol{T}}^T = \boldsymbol{I} \tag{B1}$$

Then Eq. (15) can be rewritten as

$$\boldsymbol{S}\begin{pmatrix} \boldsymbol{y} \\ \boldsymbol{x} \end{pmatrix} = \boldsymbol{S}(\boldsymbol{T}\boldsymbol{T}^T + \bar{\boldsymbol{T}}\bar{\boldsymbol{T}}^T)\begin{pmatrix} \boldsymbol{y} \\ \boldsymbol{x} \end{pmatrix} = \boldsymbol{d} \tag{B2}$$

It is clear that the matrix $\boldsymbol{T}$ stands for the selection matrix of the first $n + \nu + 1$ linearly independent columns of the matrix $\boldsymbol{S}$, then $\boldsymbol{ST}$ is a nonsingular matrix and Eq. (B2) becomes

$$\boldsymbol{T}^T\begin{pmatrix} y \\ x \end{pmatrix} = (\boldsymbol{ST})^{-1}\boldsymbol{d} - (\boldsymbol{ST})^{-1}\boldsymbol{S}\bar{\boldsymbol{T}}\bar{\boldsymbol{T}}^T\begin{pmatrix} y \\ x \end{pmatrix} \tag{B3}$$

By defining

$$z = \bar{\boldsymbol{T}}^T\begin{pmatrix} y \\ x \end{pmatrix} \tag{B4}$$

multiplying on the left side of Eq. (B3) by $\boldsymbol{T}$ and making use of identity (B1) we obtain

$$\begin{pmatrix} y \\ x \end{pmatrix} = \boldsymbol{T}(\boldsymbol{ST})^{-1}\boldsymbol{d} + (-\boldsymbol{T}(\boldsymbol{ST})^{-1}\boldsymbol{S}\bar{\boldsymbol{T}} + \bar{\boldsymbol{T}})z \tag{B5}$$

□

References

[1]Northcutt, J. D., Jensen, E. D., Burke, E. J., Clark, R. K., and Hanko, J. G., "Decentralized Computing Technology for Fault-Tolerant, Survivable C3I Systems," Carnegie-Mellon Univ., Final Rept., Pittsburgh, PA, Aug. 1985–Dec. 1988.

[2]Howell, W. E., Bundick, W. T., Hueschen, R. M., and Ostroff, A. J., "Restructurable Controls for Aircraft," AIAA Paper 83-2255, Aug. 1983.

[3]Rubertus, D. P., "Self-Repairing Flight Control Systems—Overview," *Proceedings of the National Aerospace and Electronics Conference*, Institute of Electrical and Electronics Engineers, New York, Vol. 2, 1983, pp. 1280–1286.

[4]Patton, R., *Fault Diagnosis in Dynamic Systems. Theory and Applications*, Prentice-Hall, Englewood Cliffs, NJ, 1989.

[5]Cavallo, A., Celentano, G., and De Maria, G., "Robust Stability Analysis of Uncertain Linear Time Invariant Dynamical Systems," *Proceedings of the 28th CDC*, IEEE, New York, 1989, pp. 447–451.

[6]Cavallo, A., Celentano, G., and De Maria, G., "Robust Stability Analysis of Polynomials with Linearly Dependent Coefficients Perturbations," *IEEE Transactions on Automatic Controls*, Vol. AC-36, No. 3, 1991, pp. 380–384.

[7]Youla, D. C., Jabr, H. A., and Bongiorno, J. J., "Modern Wiener-Hopf Design of Optimal Controllers, Part II," *IEEE Transactions on Automatic Control*, Vol. AC-21, No. 3, 1976, pp. 319–338.

[8]Celentano, G., and De Maria, G., "A New Linear Parameterization of All Stabilizing Compensators for Single Input Single Output Plants," *IEE Proceedings*, Vol. 136, Pt. D, No. 5, New York, 1989, pp. 225–230.

[9]Dorato, P. (ed.), *Robust Control*, IEEE Press, New York, 1987.

[10]Ackermann, J., "Parameter Space Design of Robust Control Systems," *IEEE Transactions on Automatic Control*, Vol. AC-25, No. 6, 1980, pp. 1058–1072.

[11]Kharitonov, V. L., "Asymptotic Stability of an Equilibrium Position of a Family of Systems of Linear Differential Equations," *Differential Equations*, Vol. 14, 1979, pp. 1483–1485.

[12]Ackermann, J., "Robust Control System Design," AGARD-AG-289, 1987.

[13]Ackermann, J., "Robustness Against Sensor Failures," *Automatica*, Vol. 20, No. 2, 1984, pp. 211–215.

[14]Etkin, C., *Dynamics of Atmospheric Flight*, Wiley, New York, 1972.

[15]Roskam, J., *Airplane Flight Dynamics and Automatic Flight Controls*, Parts I, II, Roskam Aviation and Engineering Corp., Ottawa, KS, 1982.

[16]Cavallo, A., De Maria, G., and Verde, L., "Robust Analysis of Handling Qualities in Aerospace Systems," *Proceedings of the 11th IFAC World Congress 1990*, Tallinn, Estonia, Vol. 5, edited by V. Utken and Ü. Jaaksoo, Pergamon, Oxford, pp. 70–75.

[17]Cavallo, A., De Maria, G., and Verde, L., "Robust Parameter Design of Flight Control Systems," *Application of Multivariable System Techniques,* edited by R. Whalley, Elsevier, London, 1990, pp. 256-263.

[18]Hartmann, U., and Lonn, E., "Anwendung der Polfestlegung beim Entwurf von Stabilisierungs systemen am Beispiel der Flugzeuglängsbewegung," *Zeitschrift für Flugwissenschaften und Weltraumforschung*, Vol. 1, No. 1, 1977, pp. 135–147.